Visual Abstract

Flexural behavior of delta and bi-delta cold-formed steel beams: experimental investigation and numerical analysis

Yazid Hadidane, Nadia Kouider
Civil Engineering Laboratory (LGC), Badji Mokhtar- Annaba University, P. O. Box 12, 23000 Annaba, Algeria; yazid.hadidane@univ-annaba.dz; y.hadidane@gmail.com
nadia.kouider@univ-annaba.dz; nadia.kouider23@gmail.com

Mohammed Benzerara
Badji Mokhtar Annaba University, LGC laboratory (Laboratory of Civil Engineering), Algeria
mohammed.benzerara@yahoo.com

ABSTRACT. Cold-formed steel (CFS) structural members retain their preferred position in the lightweight construction industry, which is due to their significant advantages. The optimization of these CSF elements will make it possible to construct buildings at very competitive prices, having in addition an increased load capacity, and thus obtaining a stable and economical construction. The main objective of this research being the evaluation of the effectiveness of these new sections in (CSF) and the estimation of the remarkable instabilities as well as the failure modes. This article deals with an experimental study on the behavior of CSF beams of delta and bi-delta shape, solicited by four-point bending loads. These cross section shapes are often used in floors as main and secondary beams. The properties of this type of sections are most often based on the method involving the effective width designated by the Eurocode 3 standard. A nonlinear analysis by finite elements (FE) using the ABAQUS calculation program is carried out, thus making it possible to compare the experimental results with the numerical ones as well as those which are given by the theory proposed by Eurocode 3. Finally, the results obtained essentially showed that the failure modes of the delta and bi-delta beams corresponded to the buckling modes local.

KEYWORDS. Cold-formed sections; Plasticity; Four-point bending test, Effective Width; Local buckling.

OPEN ACCESS

Citation: Hadidane, Y., Kouider, N., Benzerara, M., Flexural behavior of delta and bi-delta cold-formed steel beams: experimental investigation and numerical analysis, Frattura ed Integrità Strutturale, 61 (2022) 69-88.

Received: 31.01.2022
Accepted: 04.04.2022
Online first: 24.04.2022
Published: 01.07.2022

INTRODUCTION

Currently, in structural steel, structural elements used can be formed either with lime at high temperature or cold by bending simple sheets to get various desired shapes [1,2]. In practice, hot rolled sections massively used compared to cold sections [3]. However, given the current trend of building more and more resistant and lighter, CFS cold-formed profiles and especially those with thin walls are beginning to be used in the metal construction market. These types of profiles have very interesting characteristics that make them competitive, namely their lightness, ease of assembly, and the wide variety of shapes produced [4]. CFS elements have become increasingly popular in low to medium-rise multi-story buildings and CFS frames with short or intermediate spans [5]. In the field of civil engineering, cold formed steel elements are generally used in industrial buildings as purling, columns, trusses or structural elements, storage racks, vehicle bodies and various types of equipment [6,7].

For the design of these profiles, thin sheets are used, the thickness of which remains very small compared to the dimensions of the formed walls, which makes the flat parts constituting these elements more vulnerable and can become unstable under the action of the applied stresses and the weakness becomes more important if the section is used for the beam that is subjected to the bending moment [8]. Therefore, the problem of determining the critical stresses and their instability modes becomes important for the dimensioning of these types of structures.

Several studies have been conducted with the aim to understand the behavior of cold-formed thin profiles, the majority of which have resulted in three types of instabilities: local characterized by the buckling of one of these elements, global characterized by the total displacement of the section or the combination of the two types making the behavior more complex to understand [9]. The real development of the use of thin sections came only in the 1940s with the publication of the first regulations sponsorship of research by the American Iron and Steel Institute plus other codes in year 1946 [2] , the advancement of research made it possible to revise and re-edit the calculation code of these elements which allowed a more secure and economical calculation.

Other work has addressed this type of structure and some results have also led to the development of cold-formed calculation codes such as the Eurocode. However, these codes remain insufficient to understand the behavior of this type of structure and further work is needed.

Experimental tests and numerical work on the local and global stability of thin steel sections subjected to a bending moment have been studied. The data on bending capacity obtained from the studies were compared with formulas of certain codes. From the experiments, it was found that fracture initiated by distortion buckling resulted in a higher strength reduction factor than fracture [8].

There is very few codes for the design of cold-formed steel beams against bending [10]. The Australian standard AS/NZS 4600 is dedicated to cold-formed steel structures, which do not consider the torsional effect [11]. In 1946, George Winter introduced the notion of equivalent width (or effective width) on cold-formed steel members allowing local buckling to be taken into account in a simple way. When a stiffened element is subjected to a compressive force in the direction of these stiffened edges, the stresses generated by this force are not distributed uniformly over the width of this element, but in proportion to the resistance and the relative rigidity on the edges they apply. For the purpose of simplification, George Winter proposed to calculate the constraint which reigns on the edges by supposing that this one is applied on an equivalent width of dimension lower than the real width [12].

The AISI 2007 edition of the North American Specification for Cold Formed Steel Structural Members, includes new design rules for lateral unrestrained bending members subjected to bending and torsional loads [13]. These standard states that the bending resistance should be reduced by multiplying it by a reduction factor R, which is defined as the ratio between the normal stress due to bending alone and the combined stress due to both bending and torsion at the point of maximum combined stress on the cross section. Eurocode 3 Part 1.3 includes design rules for cold-formed steel structures (EN 1993-1-3, 2006) and it takes into consideration the effects of torsion when loads are applied eccentrically from the center of cross-sectional shear [10,14].

Depending on the intended use, the profiles of CFS can be open or closed, symmetrical or asymmetrical, simple or complex. This complexity depends on a certain number of factors, the number and radii of the folds, the angle formed between them by the faces, relative width of the faces according to their position and the thickness of the product. In this context,

this study refers to the design of a complex section of cold-formed steel to obtain the best properties of the open section of delta form, which undergo certain modes of instabilities, or bi-delta to ensure local and global stabilities. The first combination is to study the behavior of an open delta-shaped section, which can be mainly secondary beams (purlins, joists, etc.).

The second is the superposition of the two delta shaped sections to form a cross section bi-delta that can be used as main elements (posts, beams…). Bending beams are the most basic and common elements in steel construction. A variety of profile shapes and beam types can be used depending on the span of the member and the amount of loading.
The main objective of this research is to study the behavior of cold-formed steel beams subjected to four-point bending with lateral restraints. An experimental study plus numerical models were developed to simulate the behavior and strength of cold-formed steel beams. Non-linear analysis, including the effects of large deformation and plasticization of the material plus the notion of effective widths for class 4 sections according to Eurocode 3, have been taken into consideration. This article presents the essential details of this research and the important results found.

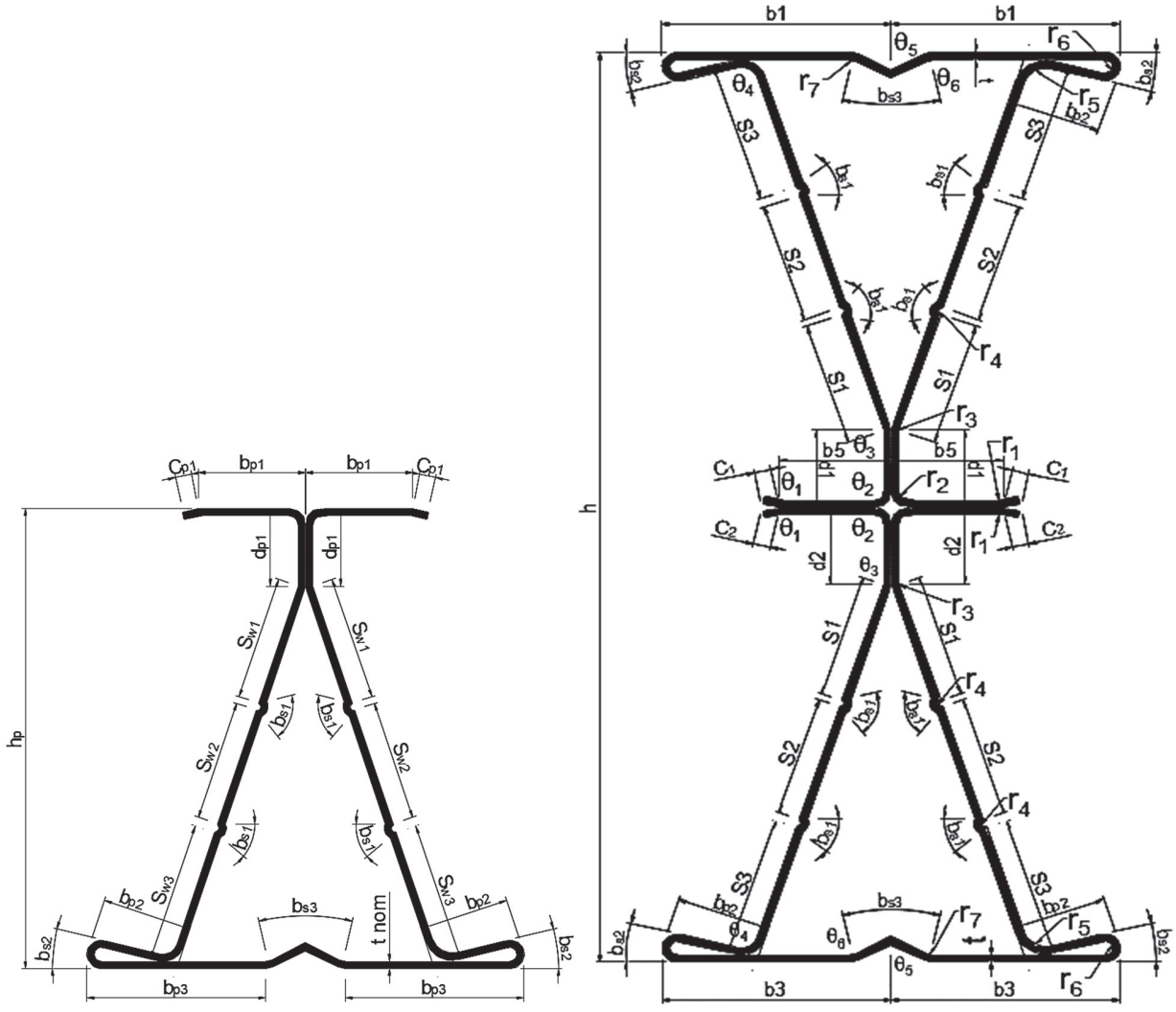

Figure 1: Beam Cross-Sections, (a) delta section and (b) bi-delta section.

THEORETICAL METHOD

In order to study the state of deformations, displacements and stresses of the studied specimens, the determination of the geometrical and mechanical characteristics of the studied sections which are cold-formed isostatic beams (delta and bi-delta) and the material used is more than necessary. For this, the notion of an effective section must be introduced taking into account the stiffeners and roundings which are present in our sections, Eurocode 3 part 1.3 is used.
Fig. 1 shows the cross-sections of the studied beams of delta and bi-delta shape obtained from cold profiling on an appropriate bending line. The beams are simply supported with 3.5 m span and 2 mm thickness with hs: the height of the

delta beam (hs=129 mm). hp: the height of the bi-delta beam (hp=258 mm). Tab. 1 summarizes all beam dimensions based on Eurocode 3.

Index	b_i (mm)	C_i (mm)	d_i (mm)	S_i (mm)	θ_i (°)	r_i (mm)	b_{si} (mm²)
1	62.40	5.60	21.00	36.00	168	1.90	14.30
2	25.80	5.60	21.00	36.30	90	1.90	22.30
3	62.40	-	-	40.10	161	5.10	38.70
4	25.80	-	-	-	95	3.30	-
5	29.60	-	-	-	128	3.20	-
6	-	-	-	-	154	2.30	-
7	-	-	-	-	-	16.10	-

Table 1: The geometric properties of sections delta and bi-delta.

Checking the dimensions in Fig. 1 and geometric proportions are based on Eurocode 3 as shown in the following conditions:

$$1.0 \text{ mm} \leq t_{cor} \leq 4.0 \text{ mm} \quad (1)$$

$$b_1/t \leq 60 \quad (2)$$

$$b_2/t \leq 60 \quad (3)$$

$$b_3/t \leq 60 \quad (4)$$

$$h_p/t \leq 500 \quad (5)$$

with t: Section thickness.
The cross section of the beams tested contains several roundings, which is why the following two conditions must be satisfied:

$$r_i/t \leq 5 \quad (6)$$

$$r_i/b_{pi} \leq 0.15 \quad (7)$$

with r_i : Ply radius;
For the delta section and the bi-delta section, the roundings (r_1, r_2, r_3, r_4, r_5 and r_6) are neglected and the rounding (r_7) must be taken into account in the calculation of the effective sections.
For the delta section and the bi-delta section, the roundings (r_1, r_2, r_3, r_5) are neglected and the rounding (r_7) must be taken into account in the calculation of the effective sections.
The cold-formed delta and bi-delta beams are class 4, these cross sections contain several roundings. the properties of the effective cross-sections are based on the theory of the method of effective widths designated by Eurocode 3 [5,14,15].
The modulus of elasticity of the effective section W_{eff} is based on an effective cross-section subjected only to a bending moment along the main axis in question, with a maximum stress σ max, Ed equal to f_{yb} / γ_{M_1}, taking into account the effects of local buckling.
The stress ratio $\Psi = \sigma_i / \sigma_s$ used for the determination of the effective parts of the web can be obtained by using the effective area of the compression flange and, on the other hand, the gross area of the web (Fig. 2).

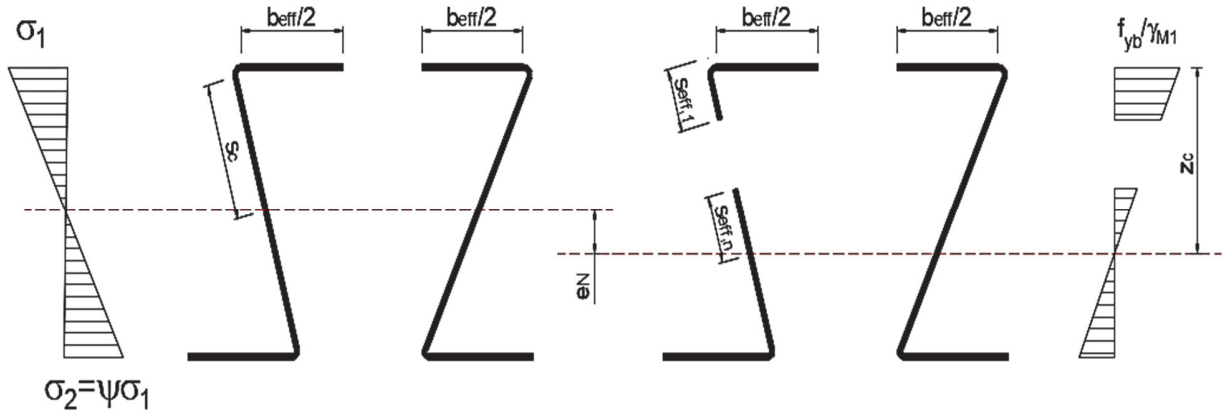

Figure 2: Effective cross section for resistance to bending moments [14].

Resistance modulus of the effective section with respect to the compression flange and the tensioned compression flange:

$$W_{eff,y,c} = \frac{I_{eff,y}}{Z_c} \tag{8}$$

$$W_{eff,y,t} = \frac{I_{eff,y}}{Z_t} \tag{9}$$

W_{eff} is the effective modulus of the cross section taking into account local buckling or distortion [5]. The average elastic limit f_{ya} of a cross-section, after cold forming, can be determined from the results of tests on a complete section in accordance with the provisions of Eurocode 3 part 1.3. Alternatively, the average increased yield stress f_{ya} can be calculated using the following formula [14]:

$$f_{ya} = f_{yb} + \frac{\left(f_u - f_{yb}\right).k.n.t^2}{A_g} \tag{10}$$

$$f_{ya} \le \frac{\left(f_u + f_{yb}\right)}{2} \tag{11}$$

A_g: the gross cross-sectional area.
K: numerical coefficient depending on the type of forming in the way k = 7.
n: number of 90° bends in the cross section with radius r ≤ 5t (bend angles less than 90° should be taken into account as fractions of n).
Local buckling effects can be assessed using the concept of effective width, slightly stressed regions in the center are ignored, as they are less effective in resisting the applied stresses. Regions near supports are much more effective and are taken to be fully effective. The behavior of the section is modeled based on the effective width. The effective width, (b_{eff}) multiplied by the edge tension (σ) is the same as the average stress in the section multiplied by the total width (b) of the compression element. The effective width of a member in compression depends on the magnitude of the applied stress fc, the width to thickness ratio of the member and the edge support conditions (Fig. 3).
The bending resistance is the resisting moment of a cross-section subjected to bending along a principal axis and must be obtained as follows [14]:

$$M_{sd} \le M_{c,Rd} = f_y \times \frac{W_{eff}}{\gamma_{M_0}} \tag{12}$$

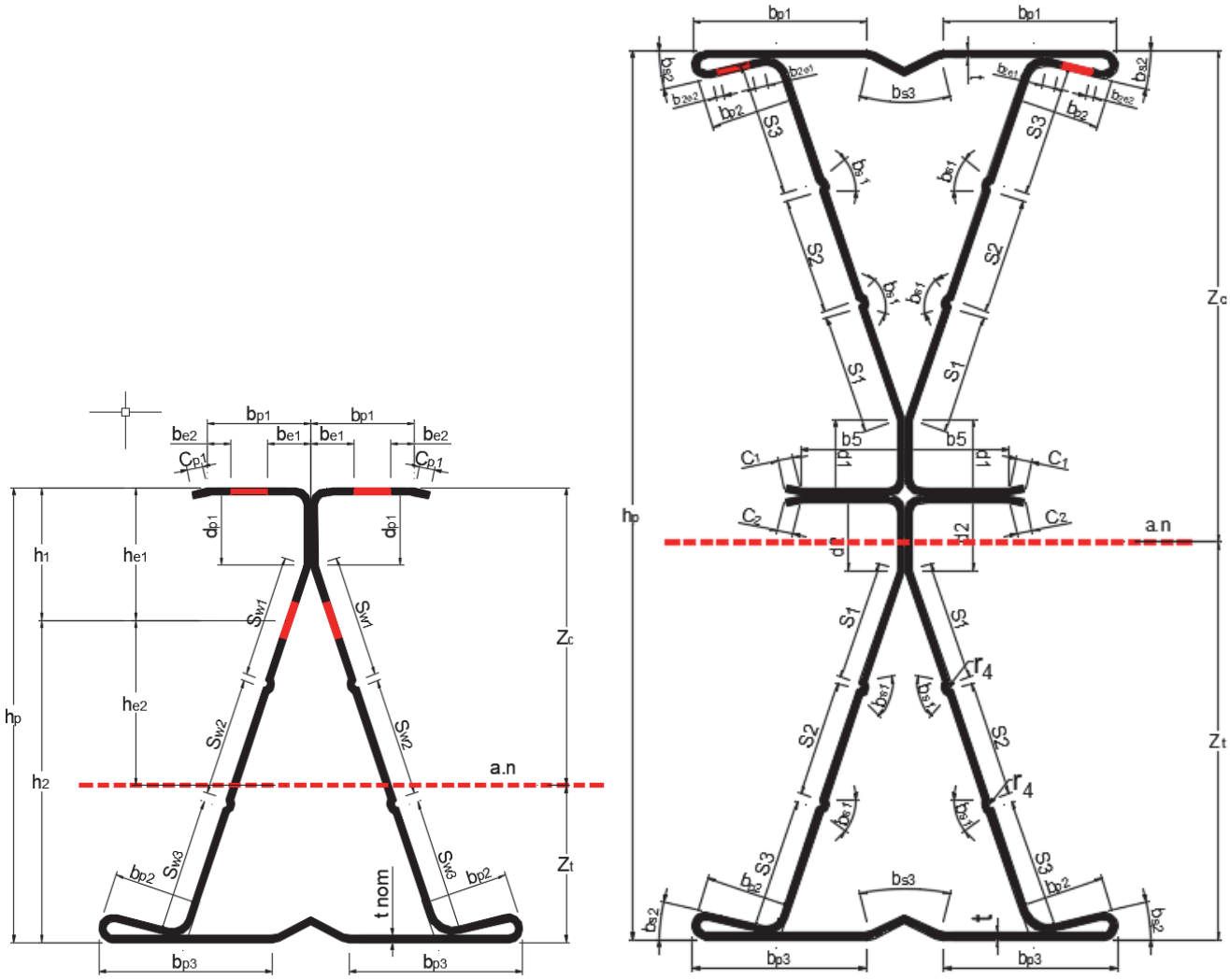

Figure 3: Different effective widths of each wall constituting the gross section, the effective section with black color for (a) delta section and (b) bi-delta section.

The experimental moment capacities and were calculated using equation (12) as follows [16]:

$$M_{sd} = p_u \times a = \frac{Pu \times L}{4} \tag{13}$$

a: the distance between the support and the applied load.
L: the span of the beam.
The determination of the deflection at mid-span of isostatic beams subjected to four-point bending (two point loads, is based on a classical method valid for small displacements in the elastic region, where it has been possible to write a relation between the total load and maximum displacement [17]:

$$P = \frac{\left(48 E I_y\right)}{3aL^2 - a^3} \delta \tag{14}$$

However, justifications on the state of deformation-stress will be necessary for each use of these cold-formed products, by experiments, since their mechanical characteristics can vary according to the shape and the number of folds.

EXPERIMENTAL PROGRAM

Specimens presentation

We conducted in the laboratory of civil engineering department (Annaba, Algeria University) an experimental study on the bending behavior of a light beam on a bending frame that can support a load of 200 kN, reconstituted from plates and of cold-formed bent sheets. The beams were manufactured by a specialized company named PROSIDER (Annaba, Algeria). The schematic diagram of the 4 point bending test is made following the instructions of the NFT57-105 standard [4,18], the loading points were spaced 1400 mm for the four-point bending. A load cell was used to monitor the applied load. Central point loads were applied to each delta and bi-delta beam using a hydraulic jack. The tested beams are fitted with two pairs of lateral supports to prevent torsional lateral buckling which is shown schematically in Fig. 4 [5,19]. The tests are carried out by load stages of 5 kN. With the growth of the applied load, deformations and deflections are recorded. The beams were loaded until the samples became unstable. The load at which the specimen fails is observed and noted as the critical failure load.

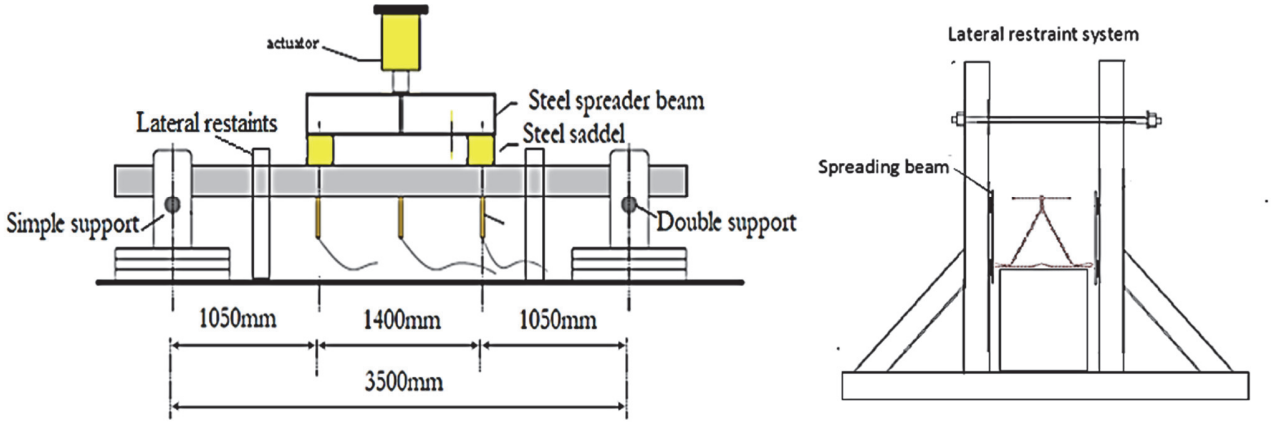

Figure 4: The schematics diagram for the experimental test and the lateral restraint system [5].

Fig. 5 brings together and clearly shows the device and the complete assembly of the measurement experiment. Since the weight of the load transmitting equipment was important for the beam specimens, a rigid steel beam was used to set two equal point loads from a jack. The weight of any equipment that has been placed above the specimen will be added later to the total maximum load to determine the beams deflection capacity.

(a) (b) (c)

Figure 5: Schematic of the experimental setup show in arrangement of vertical and lateral supports.

Test Setup

The deflections are measured using comparators, the first is placed in the middle of the bottom flange of the beam (comparator C1), and the other two are at a distance of 1050 mm from each support (comparators C2 and C3) (Fig. 6).

Strain measurements are recorded at particular locations in the cross-section of the tested specimen to provide the data needed to analyze the behavior of different reinforced systems. The deformations are measured using electric gauges [20], which are placed in the middle of the upper flange (gauge a1) and lower flange (gauge a2) of the delta and bi-delta beams. On the other hand, at web level, the a3 gauge is glued to the middle of the web height for the delta beam and to a quarter of the web height of the bi-delta beam. (Fig. 7). The gauge factor is K=2.09. Strain readings are driven by a ten ways strain gauge bridge (Fig. 7).

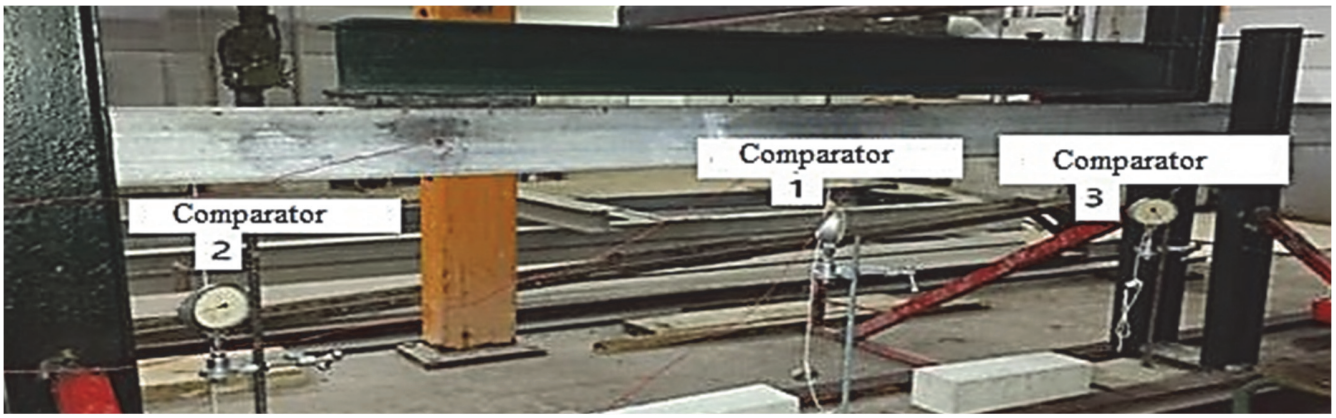

Figure 6: The location of the comparators for the experimental study.

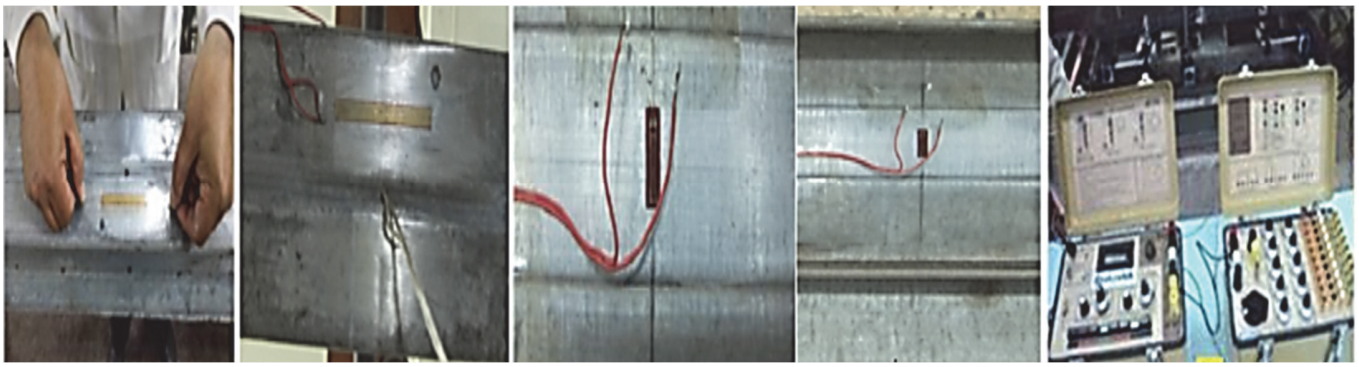

(a) (b) (c) (d) (e)

Figure 7: Bonding of gauges for experimental study: (a) at the top flange; (b) at the bottom flange; (c) at the web of the delta beam; (d) at the bi-delta web and (e) extensometer bridge.

The mechanical properties of the steel material are identified by tensile testing of six specimens, cut from flanges and webs of cold-formed steel beams, in accordance with ASTM A370-03 standards, the tensile length was 57 mm and the width was 12.5 mm. the tensile samples were pulled by the ZwickRoell machine (Fig. 8). The sample was subjected to a monotonous static load with a constant speed of 2 mm per minute.

The sections tested indicate that the beams are characterized by an average elastic limit (f_y) of 220 MPa and a tensile strength (f_u) of 300 MPa with a modulus of elasticity (E) of 2 x 10^5 MPa.

The results of the tensile tests are presented in Tab. 2. The material was observed to show no significant strain hardening after yield strength.

Experimental result

The tests made it possible to observe the real behavior of the beams during its loading, namely the permanent local buckling at the level of the upper flange of the two models of beam delta and bi-delta with the absence of elastic lateral buckling. The experimental results of the deformations obtained are presented on the graph in Fig. 9a for several cycles of loading [20].

In the interval from 0 to 7.5 kN the two gauges a1 and a2 represent the same behavior (curves combined), above this value (>7.5 kN), the gauge a1 placed at the level of the upper sole diverges rapidly to show a greater state of deformation compared to other gauges such as those placed at the level of the lower flange and in the web. These large deformations from the load

of 22.5 kN result in an elastic instability, which is the local buckling of the upper flange as shown in the figure. A maximum deformation of 2.94 x 10^{-3} for a load of 30 kN. A blistering is noticed in the core. The lower flange is less affected, the a2 gauge shows linearity with small deformations.

(a)

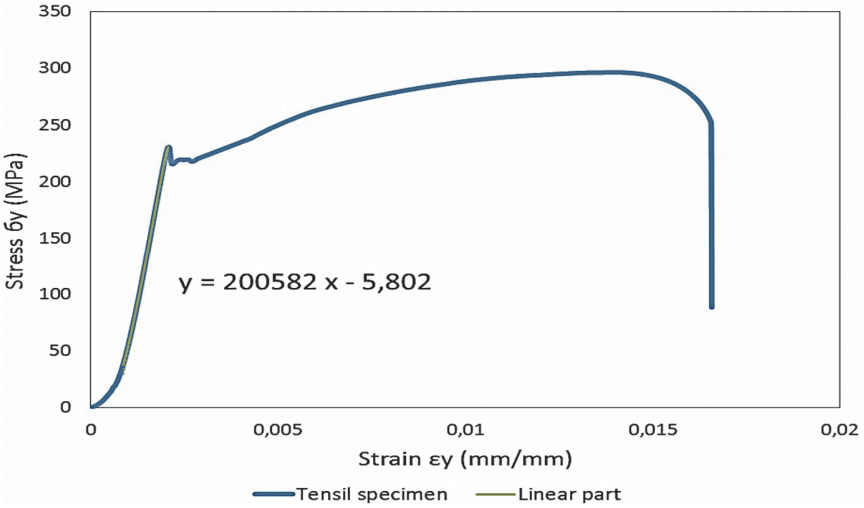

(b)

Fig.8: (a) the tensile specimen for material characterization of the delta and bi-delta beams and (b) average stress-strain curve of cold-formed steel specimens under tensile testing.

	Young's modulus E (MPa)	Elastic limit f_{yb} (MPa)	Tensile strength f_u (MPa)
Moyenne	200582	224.07	300
Ecart type	156.47	14.22	11.37

Table 2: Mechanical properties of beams.

The bending test of the delta beam shows a uniform evolution of the deflection with the increase of the load and this up to a value of 20kN from which the deflection evolved rapidly to reach a maximum value of 27mm for the comparator C1 placed in the middle of the beam (Fig. 9b).
The displacement measured by the comparator C2 is equal to 24mm and the comparator C3 is 23 mm for a load of P=30 kN. Displacements being substantially equal, one deduces from it that the applied loading is symmetrical.

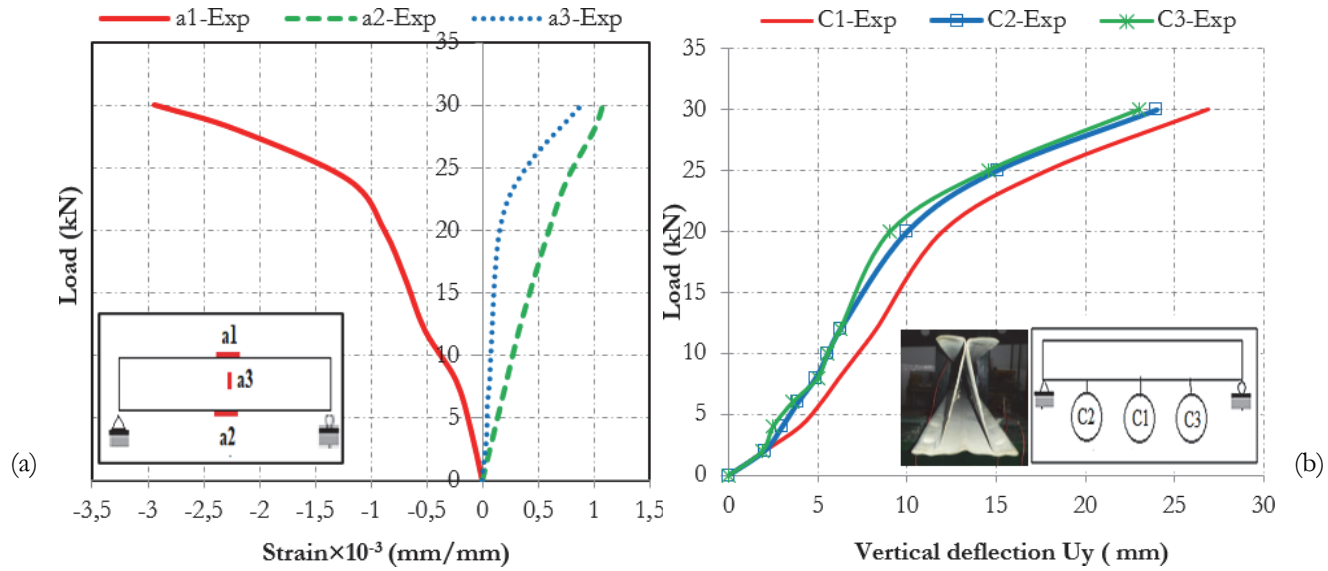

Figure 9: Experimental test results of the delta beam.

The bending test of the bi-delta beam shows significant deformations in the lower and upper flange (gauge a1 and a2), a nonlinear behavior, which is shown by a plasticization that appears from the load of 50 kN. Plasticity results in the dissipation of energy during the deformation the mechanical energy is transformed leading to the irreversibility of the behavior of the material, this mechanism also translates the ductility of the material which allows the metals to undergo significant deformations before breaking (Fig. 9a). At the end of the test, the two frames present the same deformations (the curves are confused) as shown in Fig. 10a. A maximum deformation of 1.57 x 10^{-3} for a load of 50 kN. Permanent deformation in the area of application of the load and evolve at the level of the core. The gauge (a3) positioned at the level of the web showed small deformations compared to gauges a1 and a2, a very remarkable linearity up to a load of 60 kN, and the buckling of the web appears (local deformation of the web).

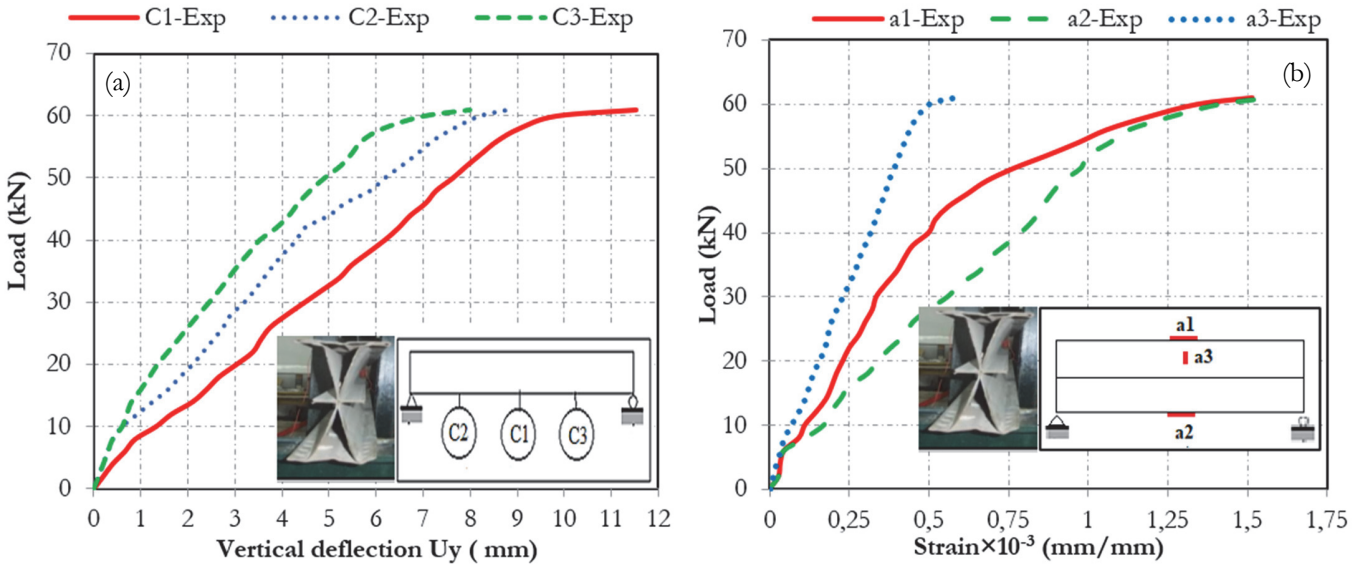

Figure 10: Experimental test results of the bi-delta beam.

The bending test of the delta beam shows a uniform evolution of the deflection with the increase of the load and this up to a value of 60 kN from which the deflection evolved rapidly to reach a maximum value of 11.5 mm for the comparator C1 placed in the middle of the beam (Fig. 9b).

The displacement measured by the comparator C2 is equal to 8.7 mm and the comparator C3 is 8mm for a load of P=60 kN. Displacements being substantially equal, one deduces from it that the applied loading is symmetrical.
The specimen returned to its original position when all fittings were removed, except for a small spot on the upper part of the mid-span sole, which suffered buckling [8].
Experimental tests have shown that the failure of cold-formed sections delta and bi- delta was obtained after local instability. This is explained by local buckling observed at the level of the upper flange, a sign of a loss of rigidity and not by the lack of resistance.

Failure mode

Tab. 3 summarizes the basic experimental results of the configurations tested in this study, the table presents the ultimate load, vertical displacement and yield moment M_y of the tested specimens.

Element	Ultimate loads (kN)	Vertical deflection Uy (mm)	Experimental moment M (kN.m)	Failure mode
Beam1 delta	30	27	6.57	Local buckling plus opening of the lips making up the top flange (in the central area) + Local buckling in load application area.
Beam2 bi-delta	60	11.54	33.56	Local buckling of top flange (load application area).

Table 3: Shear ultimate loads and failure modes.

The failure modes observed for the specimens tested can be classified into two types, the first concerning the beam delta, which represents a very remarkable local buckling in the middle section of the compressed upper flange due to the loading, conditions which prevented the free rotation of the wings during the test. With web buckling plus an opening between the edges making up the top flange (Fig. 11).
A very significant local buckling for the bi-delta beam in the areas of application of concentrated loads i.e. sinking of the upper flange with buckling of the web in these areas (Fig. 12). The study by Haris and al confirms the failure modes obtained in the open sections of cold-formed steel [8].

FINITE ELEMENT MODELLING

Finite element analysis provides a cost-effective solution to many engineering problems given the cost and time required to manufacture and create tests of actual physical models. This is why, in this article, a numerical study by finite elements is carried out using the Abaqus 6.14 software through a nonlinear structural analysis [21,22], the choice of the Abaqus software is thanks to these great performances in the numerical analysis, Finite element modeling goes through several steps starting with the creation of a geometric model of the structure, then the integration of the behavior of the material and the boundary conditions for each element which is then divided into smaller forms elements connected to specific nodes (the mesh) and analysis should be performed [4,15,23–29].

Material constitutive models

The material mechanical properties of beams have been modeled using a stress-strain model and the effect of forming and bending on the sheet will be taken into consideration in our modeling [15,30]. The material model nonlinear was defined by the actual stress-strain curve, which was derived from the tensile tests, the curve starts from the origin and has an initial slope equal to Young's modulus value $E=2\times10^5$ MPa and an elastic limit of 220 MPa in accordance with the steel constituting the delta and bi-delta beams. The Poisson's ratio is equal to 0.3.

Geometry and mesh

For the nonlinear mechanical analysis, the beams are modeled as elements of the type plates contain several folds, the mesh was chosen according to the library of ABAQUS. Concerning the beams delta (1700 elements) and bi-delta (2800 elements),

one adopted elements of nonlinear mesh of the S8R type, which is a thick hull with 8 nodes doubly curved with a reduced integration and 6 dofs/node. A finite element mesh capture of the modeled beams is presented in Fig. 13.

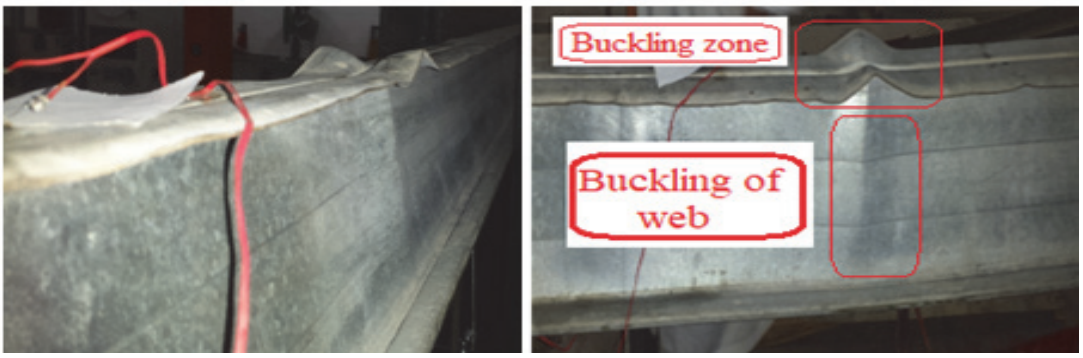

Figure 11: Failure mode of the delta beam.

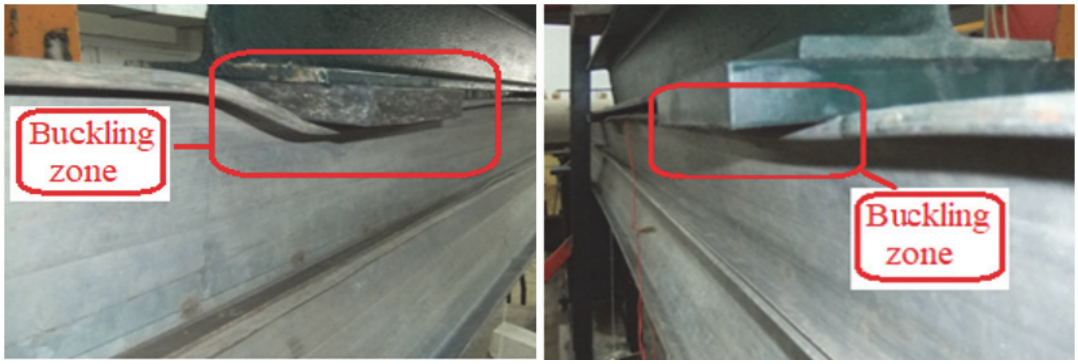

Figure 12: Failure mode of the bi-delta beam.

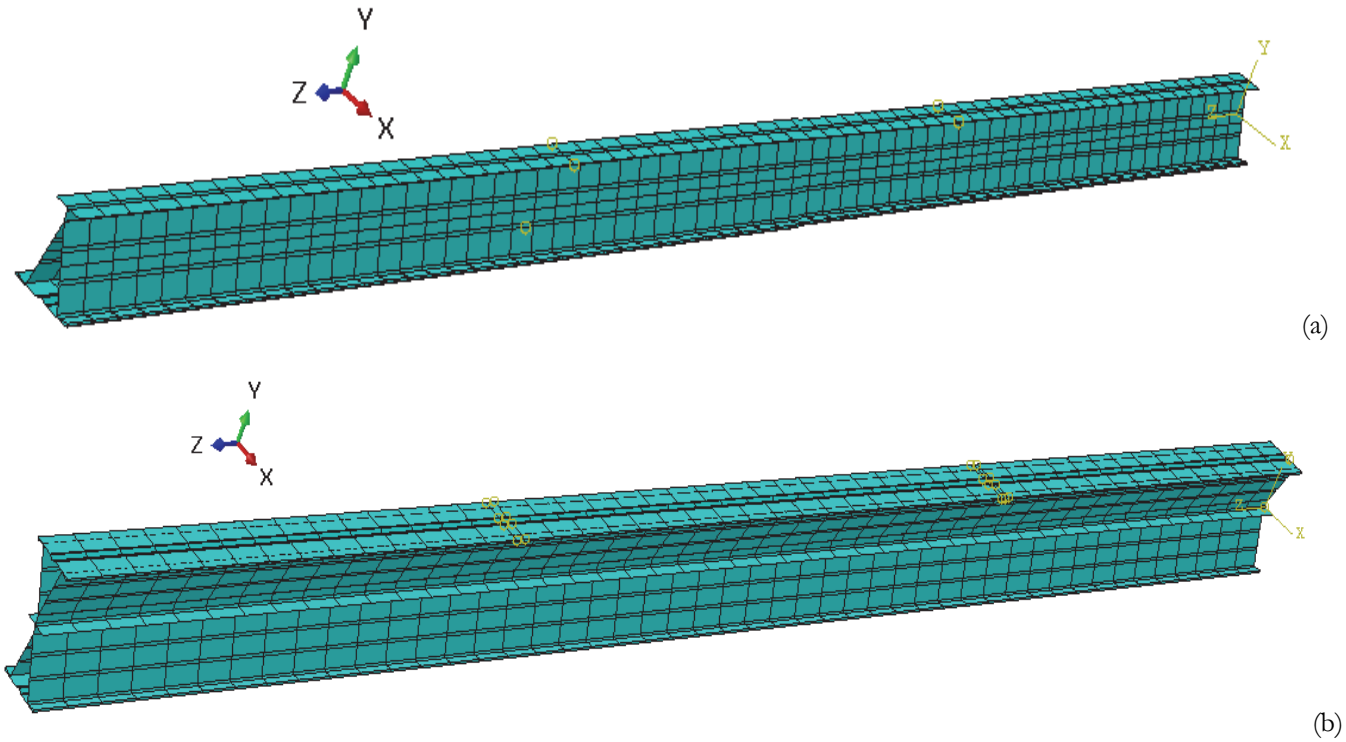

Figure 13: Finite element meshing of models, (a) delta beam and (b) bi-delta beam.

Loading and boundary conditions

The external loading of the beams tested is the four-point bending the load distribution surface has been modelled, the concentrated loads are applied at the level of the upper flange, at a distance of 1050 mm between each support. What concerned the boundary conditions, the beams tested are isostatic, the boundary conditions at the level of the first support result in a blocking of displacements in all the directions x,y,z (Ux=Uy= Uz =0). On the other hand, the other support is modeled a blocking of displacements (Ux=Uy= 0) and of rotation compared to x (Rx= 0). In addition to two pairs of side, supports to prevent lateral torsional buckling (Fig.14).

Figs. 15 and 16 show the iso-values for the delta beam such as the state of stress and displacement with the failure mode, which is already observed in the experimental study.

A very significant local buckling for the bi-delta beam in the areas of application of concentrated loads i.e. sinking of the top flange with web buckling in these areas and this is shown in Figs. 17 and 18 in stress and displacement states.

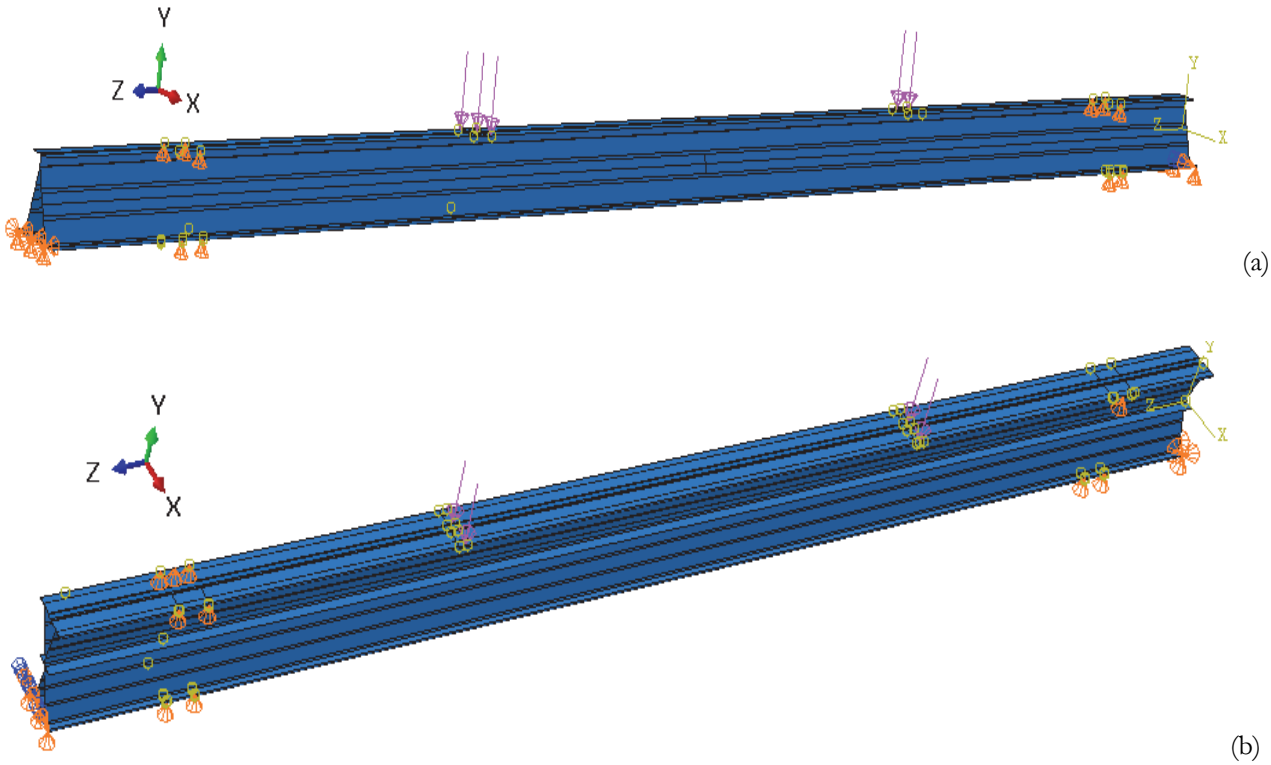

Figure 14: Boundary condition plus loading for the beams studied, (a) delta beam and (b) bi-delta beam.

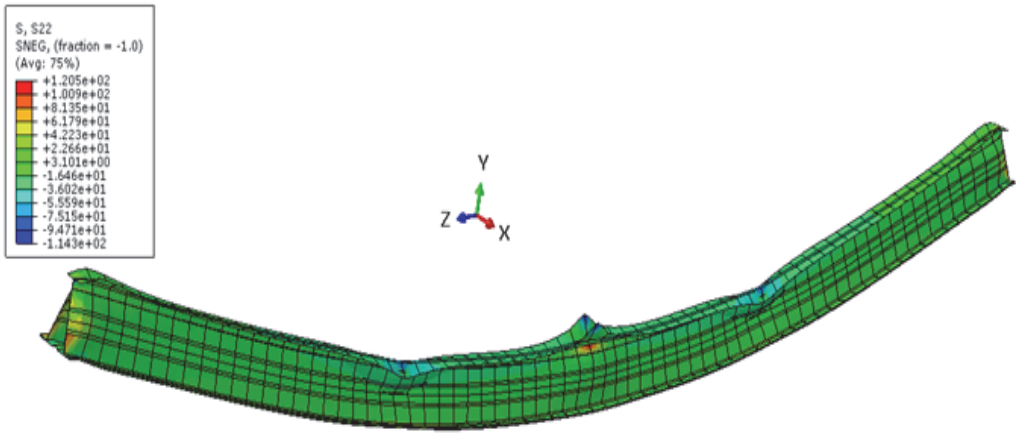

Figure 15: Failure mode (stress state) of delta beam.

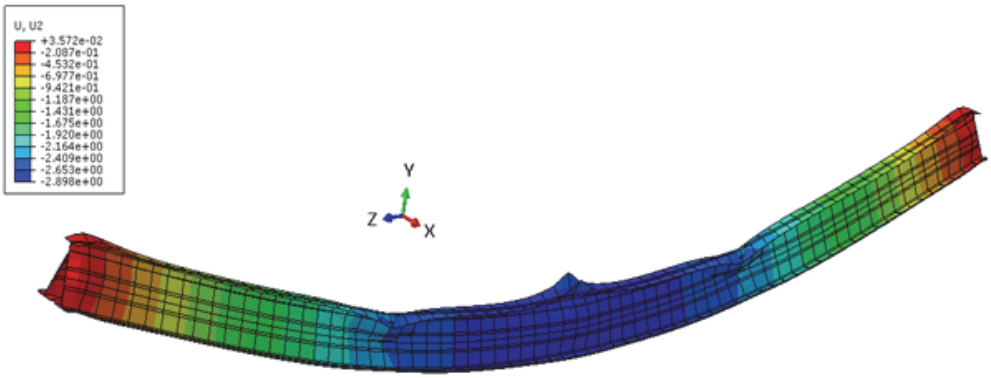

Figure 16: Failure mode (displacement state) of delta beam.

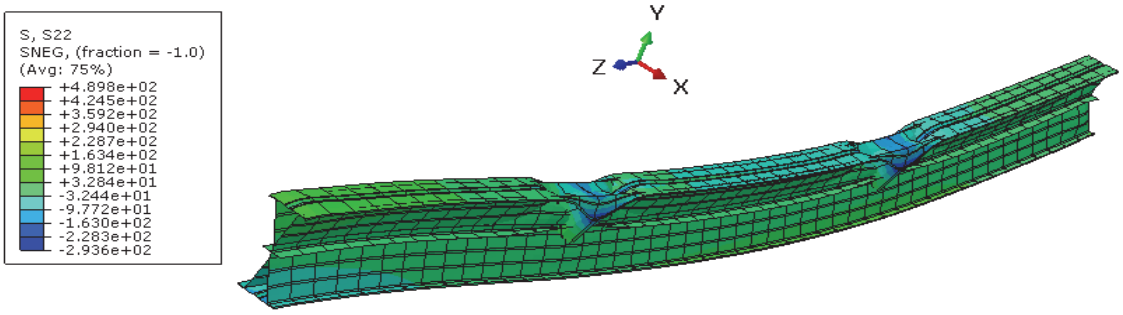

Figure 17: Failure mode (stress state) of bi-delta beam.

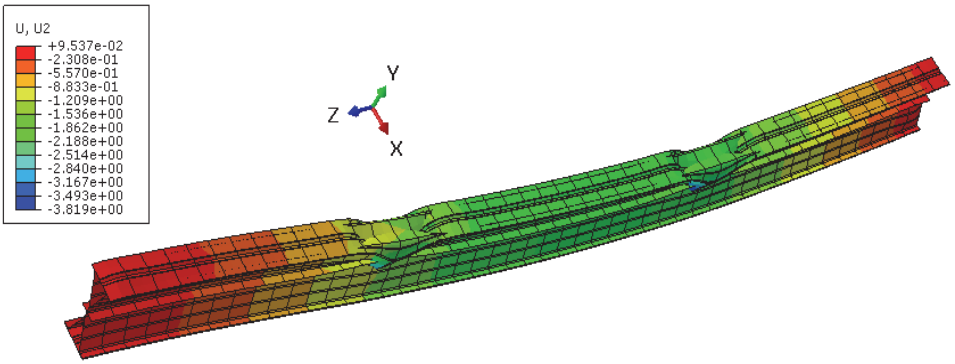

Figure 18: Failure mode (displacement state) of bi-delta beam.

RESULTS AND DISCUSSION

The ultimate capacity of the sections predicted by the FE models was on average less than 7% compared to the experimental results. The numerical results also showed that local buckling was observed in all specimens, while no lateral torsional buckling was observed, which agrees well with the tests [5] the a2 gauge shows the large deformations are in the upper and lower flanges, i.e. in the flange compressed by the presence of local buckling and in the flange stretched by the presence of maximum moments.

The three gauges have the same appearance with a non-linear behavior. The bi-delta beam shows a remarkable rigidity with small deformations thanks to the strong inertias, which represents the section (Fig. 19).

The comparison between the experimental results and the numerical predictions proves that the finite element analysis is a reliable tool to obtain fairly accurate results in a reasonable period of time. In general, the load-displacement curves were linear at the start until the maximum load was reached. The deflection increases with increasing load. (Fig. 20).

The displacements measured by the comparator C2 and the comparator C3 are very close. Displacements being substantially equal, one deduces from it that the applied loading is symmetrical. The delta beam showed great displacement especially concerning the middle comparator C1, a displacement of 27 mm for a load of 30 kN (Fig. 20).

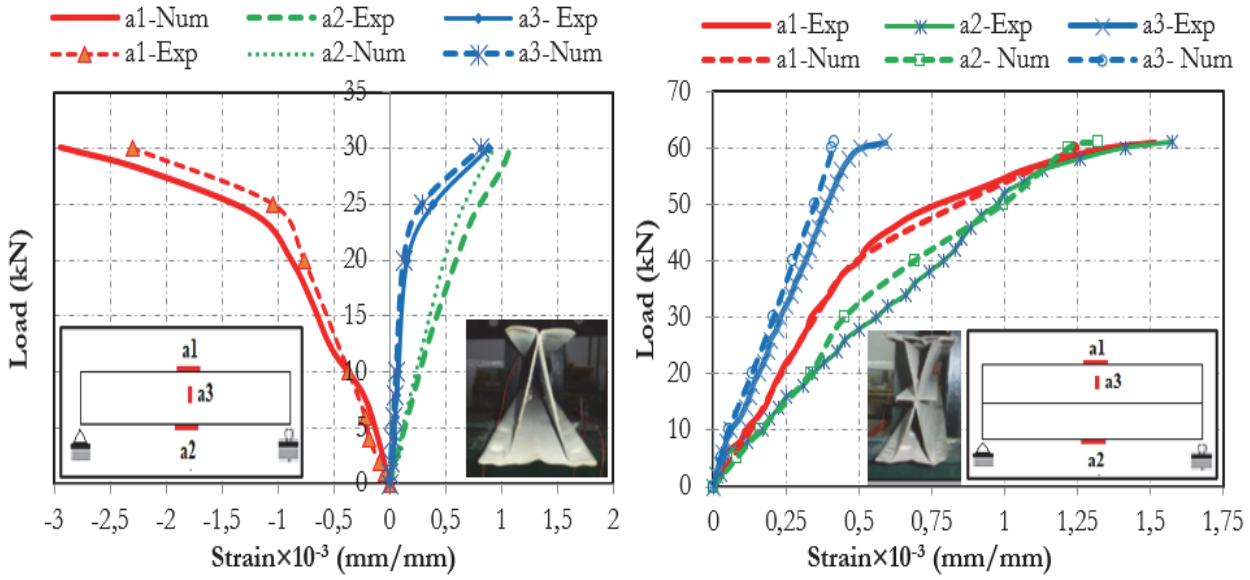

Figure 19: State comparison (load-deformation) of delta and bi-delta beams.

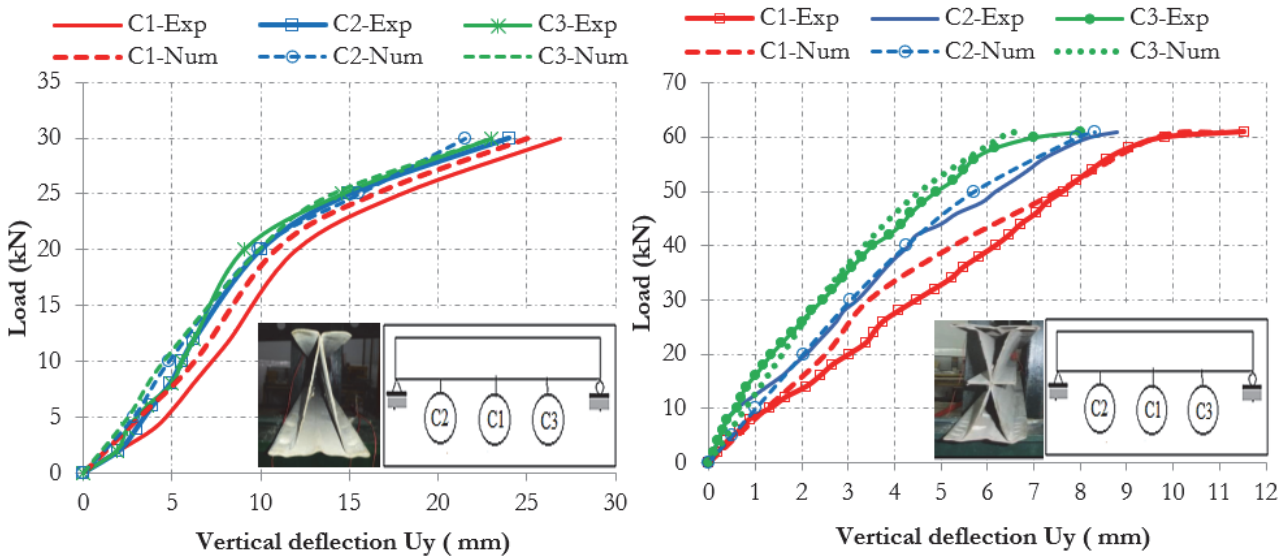

Figure 20: State comparison (load-deflection) of delta and bi-delta beams.

According to the numerical and experimental results, one notices a very good correlation between the behaviors obtained from the point of view of result and modes of ruin. Fig. 21 shows the deformation of the delta beam.
Fig. 22 presents a comparison between the expressive and numerical failure modes of the bi-delta beam. The proposed FE model was also successful in capturing failure shapes and predicting bending resistances of beams subjected to local buckling modes.
Tab. 4 and Fig. 23 show a very good correlation between the numerical results, experimental and those proposed by Eurocode 3 part 1-3 have this based on the class 4 cross section, a difference of less than 5%. The numerical results confirm that the bi-delta beam has a maximum moment capacity compared to the delta model.

Eurocode 3 gives a moment state similar to the experimental and numerical modes and the notion of the cross section is important. Therefore, it can be seen that the failure modes of the beams tested in the FE models were similar with the results of the experimental tests, which allowed us to trust the developed numerical model.

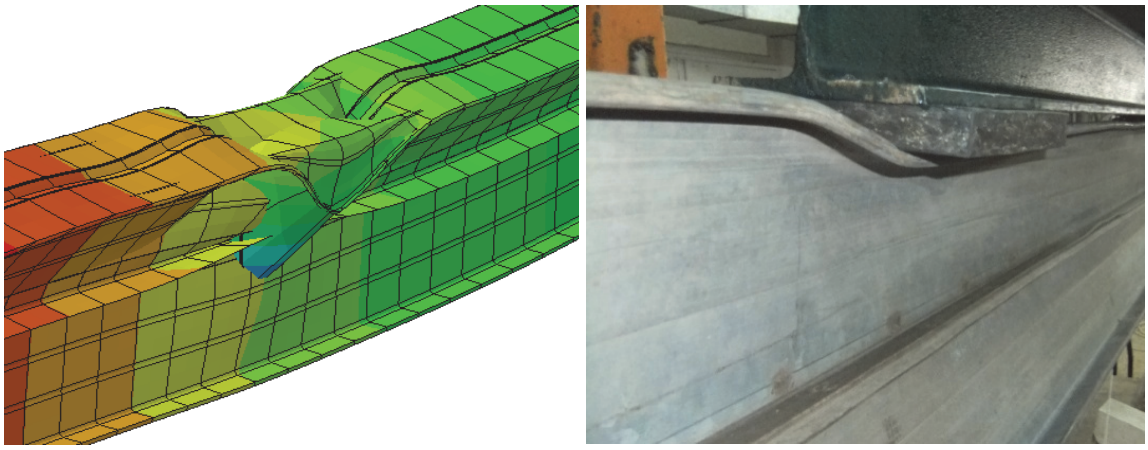

Figure 21: Stress distribution and deformations in bi-delta beam.

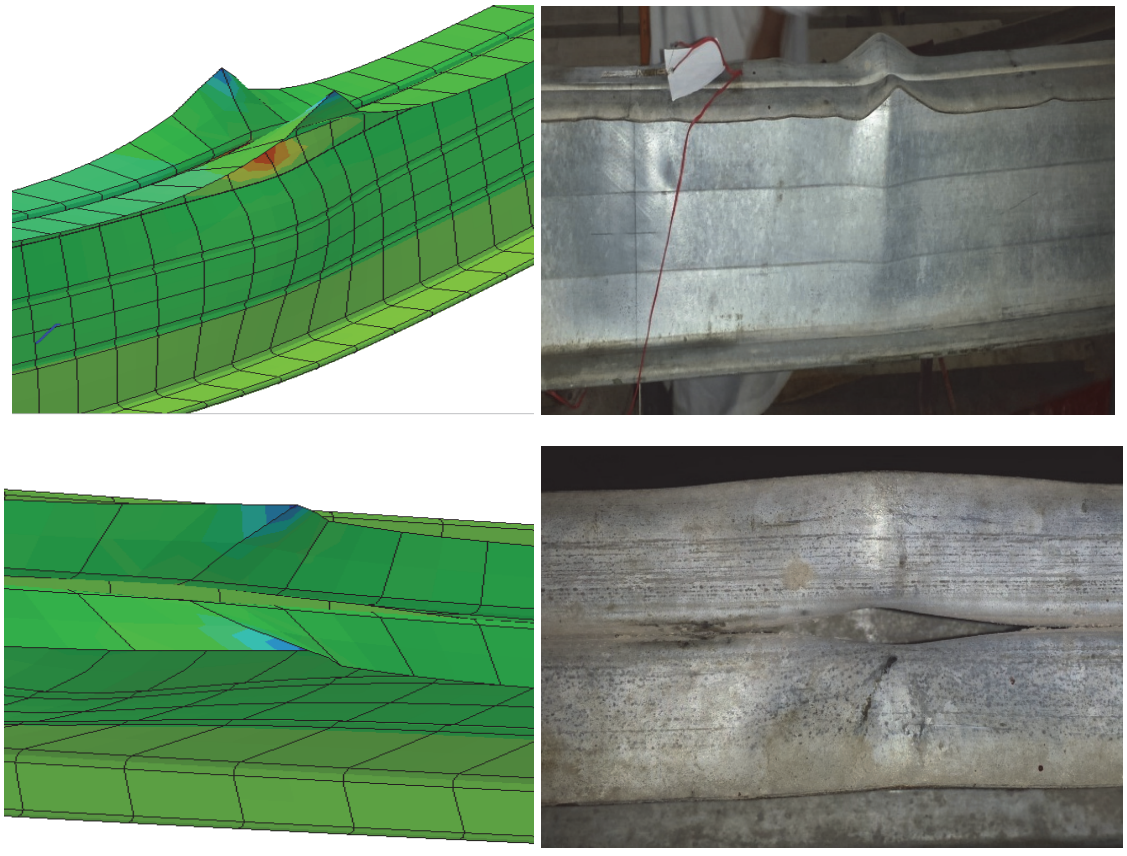

Figure 22: Stress distribution and deformations in delta beam.

Element	Experimental moment $M_{y.exp}$ (kN.m)	Numerical moment $M_{y.num}$ (kN.m)	Theoretical moment $M_{y.anl}$ (kN.m)
Beam1 delta	6.57	5.02	5.97
Beam2 bi-delta	33.56	31.95	32.28

Table 4: Comparison between experimental, numerical and analytical results.

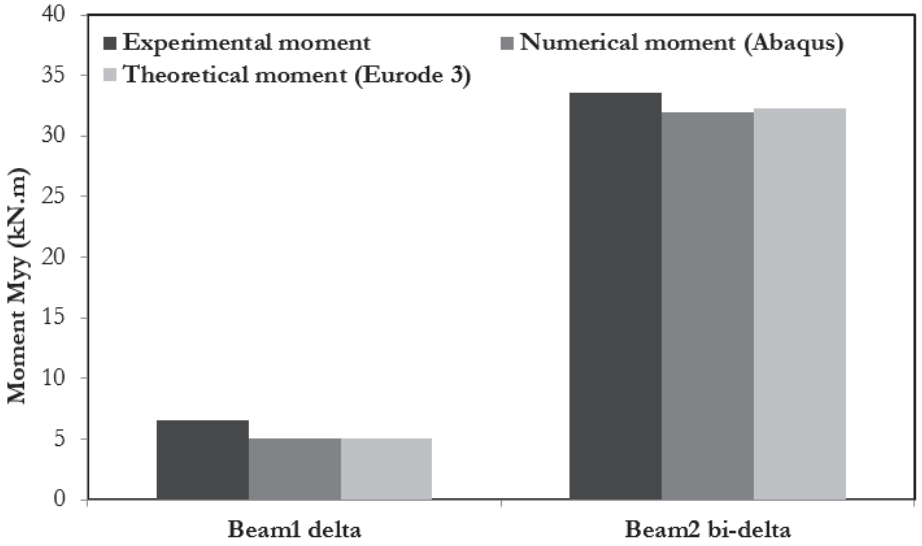

Figure 23: Comparison of experimental, numerical and theoretical maximum moments of delta and bi-delta beams.

CONCLUSIONS

The experimental tests of the delta and bi-delta beams allowed us to see the real behavior of the cold-formed beams. Numerical modeling takes into account the nonlinear behavior of the stress-strain state of the cold-formed material due to the bending effects of thin sheets plus geometric imperfections. The numerical model has been validated against an experimental program. The validated models were then used to evaluate the accuracy of effective width design methods proposed by the European standard Eurocode 3 for better design. Based on the results presented in this article, the following conclusions can be drawn:

- Buckling of the compressed upper flanges plus web buckling was observed. The FEA predictions are generally in good agreement with the experimental failure modes. The results show that local buckling has a greater influence on the strength of the specimens.
- For cold sections, when the concept of thinness appears, local buckling of the compressed walls must be considered.
- The damage was localized on the local buckling zone, while the other sections of the beam were practically unchanged. After locking onto the web, the beam has considerably lost its resistance.
- Absence of distortional local buckling thanks to the lateral support system.
- The effects of local buckling must be taken into account when determining the strength and stiffness of cold formed beams, this can be done using the characteristics of the effective cross section calculated on the basis of the effective widths of the walls which are exposed to local buckling.
- The good level of concordance of these results makes it possible to use with confidence the numerical model developed.

NOMENCLATURE

CFS: Cold-formed steel.

FE: Finite element.
h : Height of profile.
b_f : Width of flange.
t_f : Thickness of flange.
t_w : Thickness of web.
d_w : Height of web.
C: Length of dropped edge.
t : Section thickness.
h_p : Height of web.
bp_1 , bp_2 : Initial effective widths.
Cp_1 ,Cp_2 , Cp_3 , Cp_4 : Initial effective width of flanged edges.
le_1 , le_2 : Effective sole widths.
C_{eff1} : Effective width of flanged edges.
L: Length of beam.
θ : Orientation angle
f_y: The yield strength of steel.
f_u : Ultimate strength.
E: Elasticity module.
ϑ: Poisson coefficient.
b_u : ply width.
C_i : flange width.
d_i : height.
S_i : distance between plies.
θ_i : Rotation angle.
R_i : Ply radius.
b_{si} : Edge ply rotation surface.
b_{eff} : The effective width.
$M_{C, Rd}$: The calculation value of flexural strength with respect to a main axis of the section.
M_{sd} : The bending moment at the ultimate limit state.
V_{sd} : Shearing force at the ultimate limit state.
P: Concentrated load.
a: lever arm
$V_{pl, Rd}$: Design value of the plastic shear strength.
$I_{eff, y}$: Effective moment of inertia with respect to the axis (yy).
$W_{eff, y}$: Modulus of resistance cross section.
Z_c : Compressed zone.
Z_t : Tensile zone.
$\sigma_{max, Ed}$:The maximum compressive stress.
f_{yb} : Elastic limit
γ_{M_1} : Safety factor
ψ: Ratio of moments in segment.
A_g : The gross cross-sectional area.
K : Numerical coefficient depending on the type of forming.
n : Number of 90° bends in the cross section.

REFERENCE

[1] Mansuri, S., Parmar, P.K.A. (2017). Numerical investigation of flexural strength of cold form built-up beams, Int. J. Adv. Res. Sci. Eng., 6(1), pp. 109–116.

[2] Prakash, P.S., Samuel, J., Joanna, P.S., Sakaria, P.E. (2014). Flexural Behavior of Cold Formed Steel Beams with end Stiffeners and Encased Web, Int. J. Eng. Res. Technol., 3(11), pp. 1276–1279.

[3] Sumathi, A. (2017). Flexural behavior of cold formed steel i-section beam with corrugated web, Asian J. Civ. Eng., 18(1), pp. 31–38.

[4] Gatheeshgar, P., Poologanathan, K., Gunalan, S., Nagaratnam, B., Tsavdaridis, K.D., Ye, J. (2020). Structural behaviour of optimized cold-formed steel beams, Steel Constr., 13(4), pp. 294–304, DOI: 10.1002/stco.201900024.

[5] Ye, J., Mojtabaei, S.M., Hajirasouliha, I., Shepherd, P., Pilakoutas, K. (2018). Strength and deflection behaviour of cold-formed steel back-to-back channels, Eng. Struct., 177(September), pp. 641–654, DOI: 10.1016/j.engstruct.2018.09.064.

[6] Reza, W., Selvan, S.S. (2016). Experimental Study on Flexural Behaviour of Cold Formed Steel Channel and I Sections Providing Angle Stiffener on the Web, Indian J. Sci. Technol., 9(35), pp. 1–5, DOI: 10.17485/ijst/2016/v9i35/95967.

[7] Sivaranjani, S., Nalini, S., Annapurani, M. (2018). Flexural behaviour of cold form steel sections subjected to static loading, Int. J. Civ. Eng. Technol., 9(3), pp. 969–976.

[8] Haris, S., Prasetio, A., Thamrin, R., Herman, H. (2018). An experimental study of bending behaviour of double channel and hollow sections of light gauge steel, Int. J. Adv. Sci. Eng. Inf. Technol., 8(3), pp. 882–888, DOI: 10.18517/ijaseit.8.3.4192.

[9] Laím, L., Paulo C. Rodrigues, J. (2015). Flexural behaviour of cold-formed steel beams in fire situation, Rev. Estrut. Do Aço, 4(1), pp. 73, DOI: 10.17648/aco-2238-9377-4-1-5.

[10] Wan, H.X., Mahendran, M. (2016).Buckling behaviour of cold-formed steel beams under bending and torsion. Wei-Wen Yu International Specialty Conference on Cold-Formed Steel Structures, Baltimore, Maryland, U.S.A, pp. 219–33.

[11] Standards Australia SA. (2005). AS/NZS 4600, Cold-Formed Steel Struct. Sydney, Aust., ,.

[12] Descudé, M., Magniez, G. (1976). Le profilage a froid une utilisation rationnelle des produits plats en acier, Rev. Métallurgie, 73(1), pp. 13–36.

[13] American Iron. (2007). North American Specification for the Design of Cold-Formed Steel Structural Members, Am. Iron Steel Inst. (AISI). Washingt. DC, USA.

[14] Eurocode 3. (2003). Design of steel structures, Part 1.3 Gen. Rules Supplemary Cold Form. Thin Gauge Members Sheeting, CEN (European Commitee Stand.

[15] Kouider, N., Hadidane, Y., Benzerara, M. (2022). Numerical investigation of the cold-formed I-beams bending strength with different web shapes, Frat. Ed Integrità Strutt., 16(59), pp. 153–171, DOI: 10.3221/IGF-ESIS.59.12.

[16] El Refai, A., Abed, F., Al-Rahmani, A. (2015). Structural performance and serviceability of concrete beams reinforced with hybrid (GFRP and steel) bars, Constr. Build. Mater., 96, pp. 518–529, DOI: 10.1016/j.conbuildmat.2015.08.063.

[17] Buick, D., Owens, G. (2002). SteelDesignersManual6thedition, Steel Des. Man., 6, pp. 1370.

[18] Deng, J., Lee, M.M.K. (2007). Behaviour under static loading of metallic beams reinforced with a bonded CFRP plate, Compos. Struct., 78(2), pp. 232–242, DOI: 10.1016/j.compstruct.2005.09.004.

[19] Sweedan, A.M.I., Alhadid, M.M.A., El-Sawy, K.M. (2016). Experimental study of the flexural response of steel beams strengthened with anchored hybrid composites, Thin-Walled Struct., 99, pp. 1–11, DOI: 10.1016/j.tws.2015.10.026.

[20] Liu, Q. (2012).Structural analysis and design of cold formed steel sigma purlins. Doctoral thesis, University of Birmingham, GB.

[21] Ouladbrahim, A., Belaidi, I., Khatir, S., Wahab, M.A., Magagnini, E., Capozucca, R. (2021). Sensitivity analysis of the gtn damage parameters at different temperature for dynamic fracture propagation in x70 pipeline steel using neural network, Frat. Ed Integrita Strutt., 15(58), pp. 442–452, DOI: 10.3221/IGF-ESIS.58.32.

[22] Ouladbrahim, A., Belaidi, I., Khatir, S., Magagnini, E., Capozucca, R., Wahab, M.A. (2022). Prediction of Gurson Damage Model Parameters Coupled with Hardening Law Identification of Steel X70 Pipeline Using Neural Network, Met. Mater. Int., 28(2), pp. 370–384, DOI: 10.1007/s12540-021-01024-4.

[23] Dar, M.., Subramanian, N., Dar, A.., Anbarasu, M., Lim, J.B.., Atif, M. (2019). Behaviour of partly stiffened coldformedsteel built-up beams: Experimental investigation and numerical validation, Adv. Struct. Eng., 22(1), pp. 172–186, DOI: 10.1177/1369433218782767.

[24] Adel, B., Noureddine, F., Mohcene, B., Mesbah, H.A. (2020). Modeling of CFRP strengthened RC beams using the

SNSM technique, proposed as an alternative to NSM and EBR techniques, Frat. Ed Integrità Strutt., 14(54), pp. 21–35, DOI: 10.3221/IGF-ESIS.54.02.

[25] Boursas, F., Boutagouga, D. (2021). Parametric study of I-shaped shear connectors with different orientations in push-out test, Frat. Ed Integrita Strutt., 15(57), pp. 24–39, DOI: 10.3221/IGF-ESIS.57.03.

[26] Bouaricha, A., Handel, N., Boutouta, A., Djouimaa, S. (2021). Load bearing capacity of thin-walled rectangular and I-shaped steel sections of short both empty and concrete-filled columns, Frat. Ed Integrità Strutt., 15(58), pp. 77–85, DOI: 10.3221/igf-esis.58.06.

[27] Behtani, A., Tiachacht, S., Khatir, T., Khatir, S., Abdel Wahab, M., Benaissa, B. (2021). Residual Force Method for damage identification in a laminated composite plate with different boundary conditions, Frat. Ed Integrità Strutt., 16(59), pp. 35–48, DOI: 10.3221/igf-esis.59.03.

[28] Khatir, S., Wahab, M.A., Tiachacht, S., Le Thanh, C., Capozucca, R., Magagnini, E., Benaissa, B. (2021). Damage identification in steel plate using frf and inverse analysis, Frat. Ed Integrita Strutt., 15(58), pp. 416–433, DOI: 10.3221/IGF-ESIS.58.30.

[29] Allaoua, F., Lebbal, H., Belarbi, A. (2021). Finite element analysis of stress state in the cement of total hip prosthesis with elastomeric stress barrier, Frat. Ed Integrita Strutt., 15(57), pp. 281–290, DOI: 10.3221/IGF-ESIS.57.20.

[30] Wanniarachchi, S. (2005).Flexural Behaviour and Design of Cold- formed Steel Beams with Rectangular Hollow Flanges. Doctoral thesis, Queensland University of Technology (QUT), Brisbane, Australia.